Supporting Information

Understanding the Adsorption of PFOA on MIL-101(Cr)-based Anionic-exchange Metal-organic Frameworks: Comparing DFT Calculations with Aqueous Sorption Experiments

Kai Liu, Siyu Zhang, Xiyue Hu, Kunyang Zhang, Ajay Roy, and Gang Yu*

School of Environment, Beijing Key Laboratory for Emerging Organic Contaminants Control, State Key Joint Laboratory of Environment Simulation and Pollution Control (SKLESPC), Tsinghua University, Beijing 100084, China

To whom correspondence may be addressed:

Tel: +86 10 6278 1737. Fax: +86 10 6279 4006. E-mail: yg-den@tsinghua.edu.cn

Pages: 11
Figures S1-S13
Table S1

Table S1 N_2physisorption results of MIL-101(Cr), amine intermediates, and anionic exchangers MIL-101(Cr)-NMe_3 andMIL-101(Cr)-QDMEN.

MOFs	S_{BET} (m^2 g^{-1})
MIL-101(Cr)	2560
MIL-101(Cr)-DMEN	1692
MIL-101(Cr)-QDMEN	1530
MIL-101(Cr)-NH_2	1195
MIL-101(Cr)-NMe_3	445

Figure S1. PXRD patterns of(a) MIL-101(Cr), (b) MIL-101(Cr)-DMEN, (c) MIL-101(Cr)-QDMEN, (d) MIL-101(Cr)-NH_2,and (e) MIL-101(Cr)-NMe_3 after vacuum treatment 423 K for 12h.

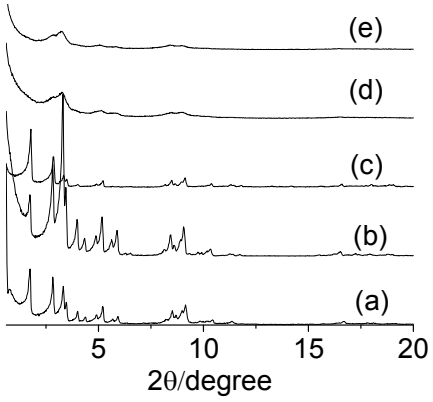

Figure S2. Infrared absorption spectra obtained from the samples: (a) MIL-101(Cr)-NMe_3, (b) MIL-101(Cr)-NH_2, and (c) MIL-101(Cr)after vacuum treatment 423 K for 12h.

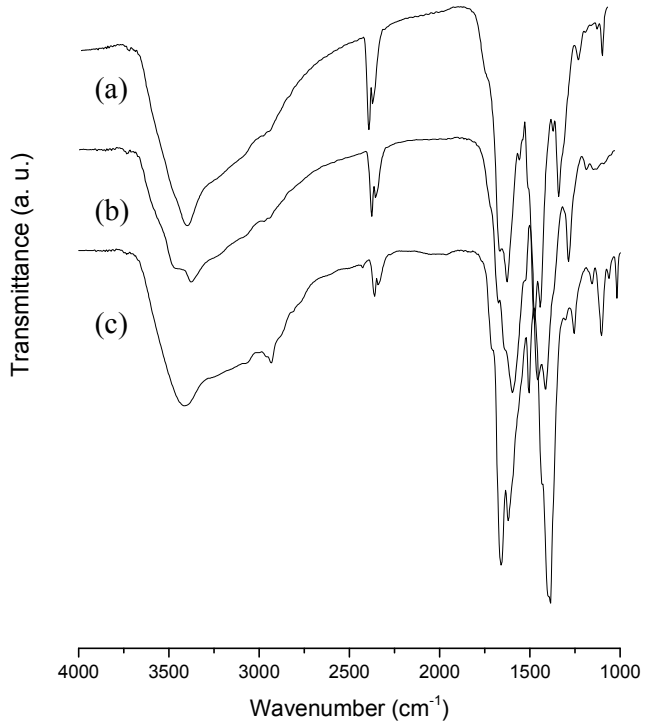

Figure S3. Infrared absorption spectra obtained from the samples: (a) liquid DMEN, (b) MIL-101(Cr)-QDMEN, (c) MIL-101(Cr)-DMEN, and (d) MIL-101(Cr)after vacuum treatment 423 K for 1h.

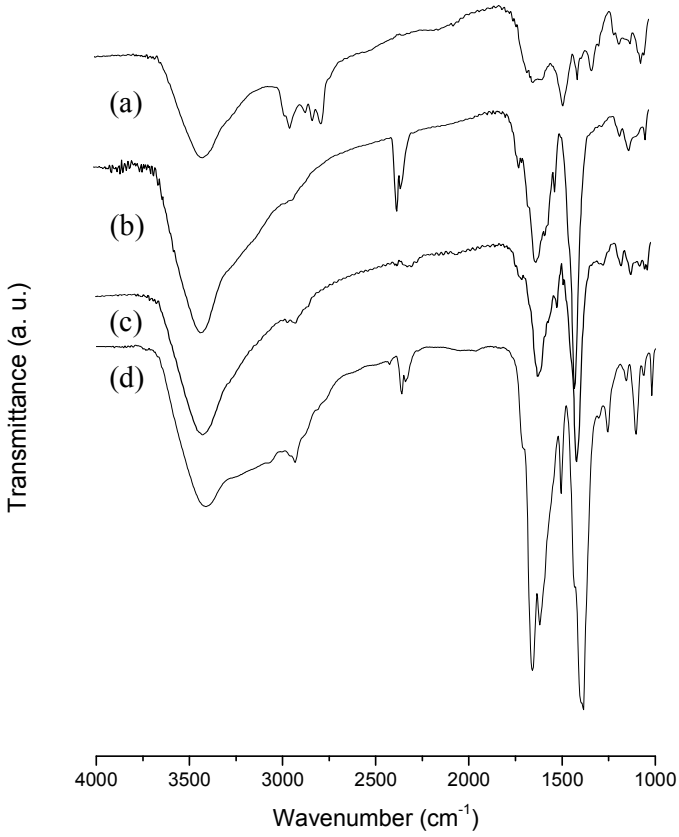

Figure S4.High-resolution XPS C1sspectra of: (a) MIL-101(Cr)-NH_2, (b)MIL-101(Cr)-NMe_3, (c) MIL-101(Cr)-DMEN, (b)MIL-101(Cr)-QDMEN,

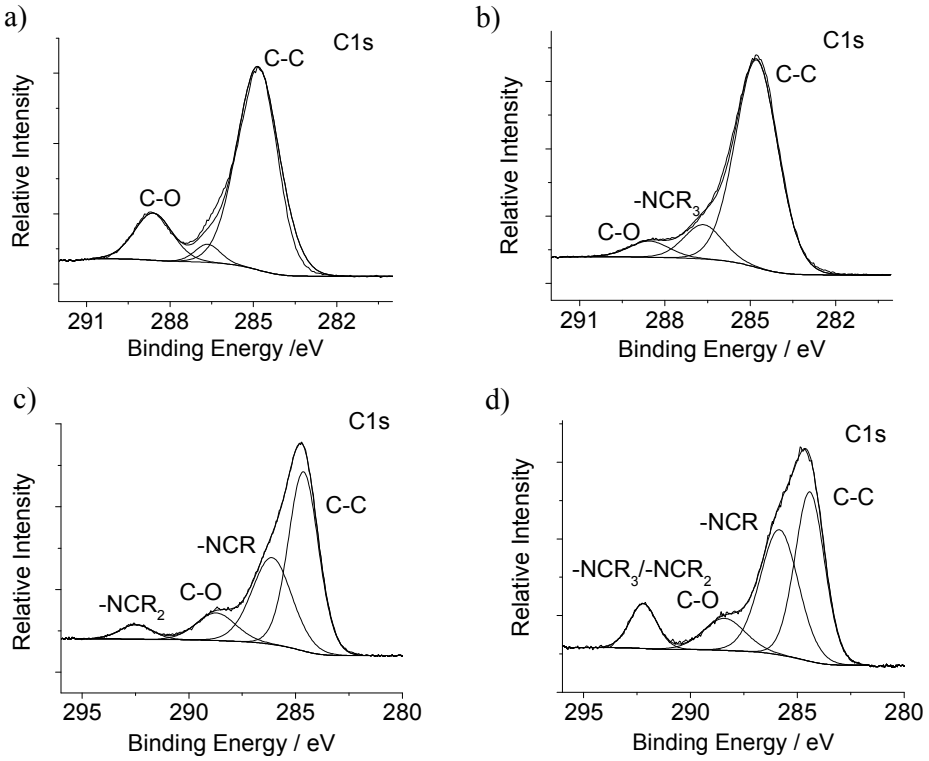

Figure S5.High-resolution XPS N1s spectra of: (a) MIL-101(Cr)-NH_2, (b)MIL-101(Cr)-NMe_3, (c) MIL-101(Cr)-DMEN, (b)MIL-101(Cr)-QDMEN,

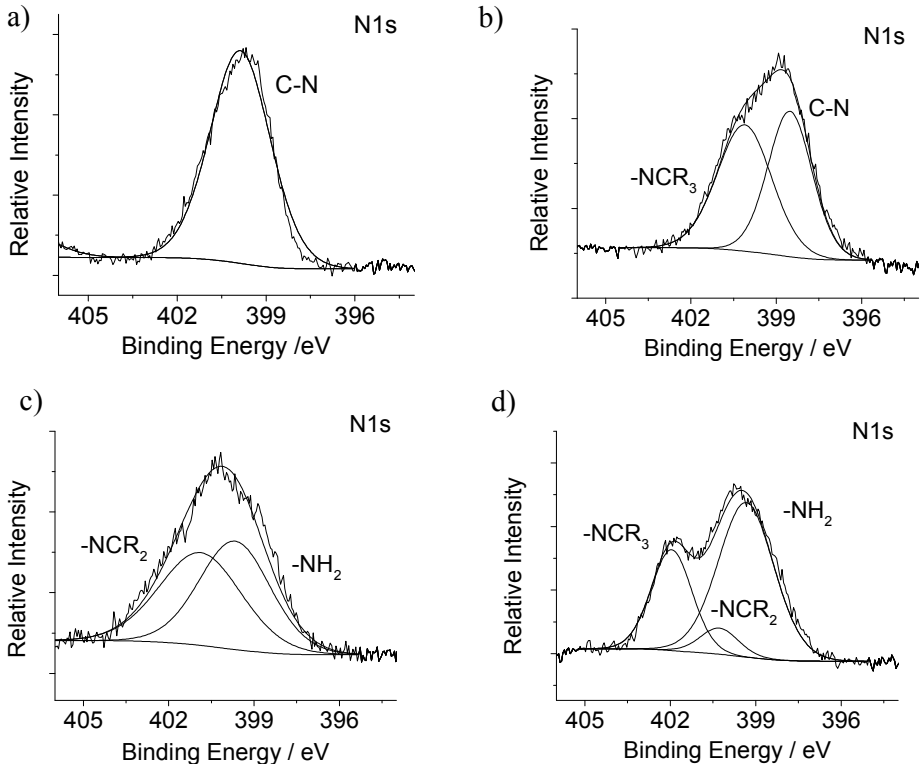

Figure S6. SEM images of(a) MIL-101(Cr), (b) MIL-101(Cr)-DMEN, (c) MIL-101(Cr)-QDMEN, (d) MIL-101(Cr)-NH_2,and (d) MIL-101(Cr)-NMe_3after vacuum treatment at 423 K for 12h.

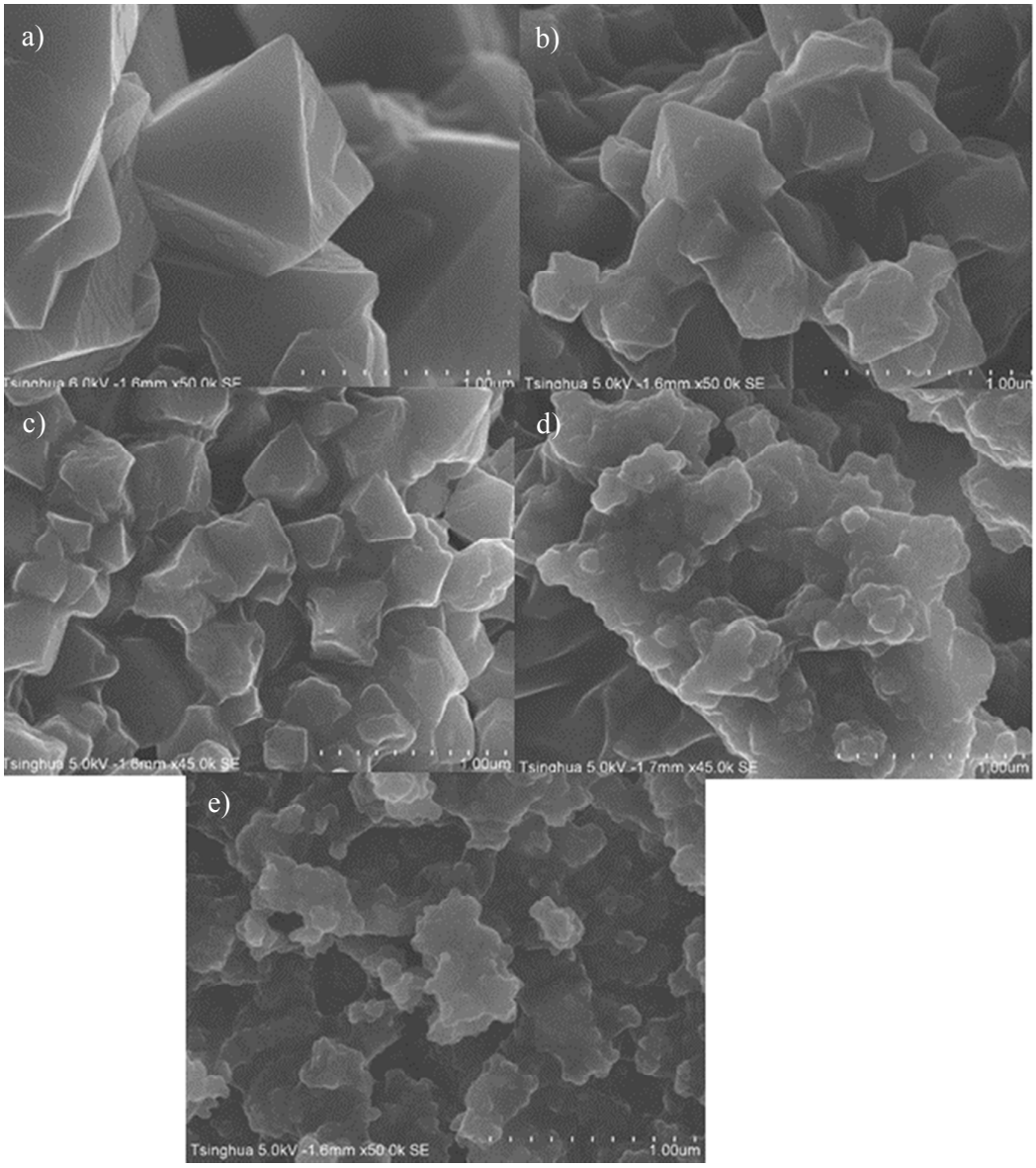

Figure S7. Adsorption isotherms of PFOA on MOFs normalized with surface area for MIL-101(Cr) (▲); MIL-101(Cr)-NH_2(■); (d) MIL-101(Cr)-NMe_3(□); (e) MIL-101(Cr)-DMEN (●); and (f) MIL-101(Cr)-QDMEN (○). Results fitted using Langmuir models.

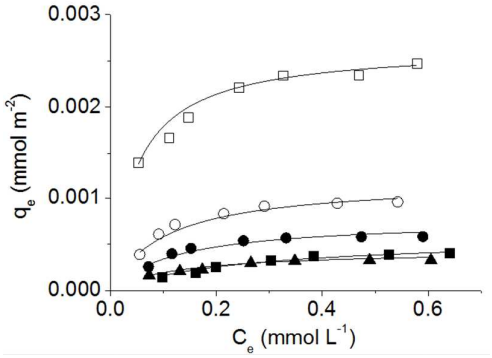

Figure S8. Removal of PFOA by MIL-101(Cr)-QDMEN in successive adsorption cycles.

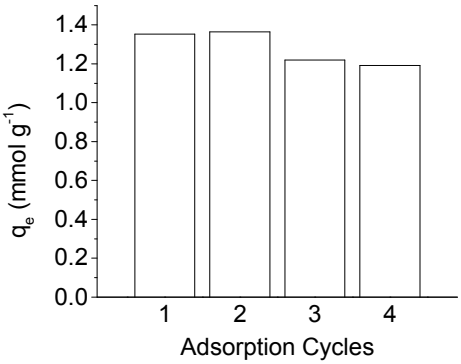

Figure S9. Infrared absorption spectra of MIL-101(Cr)-QDMEN after four adsorption cycles.

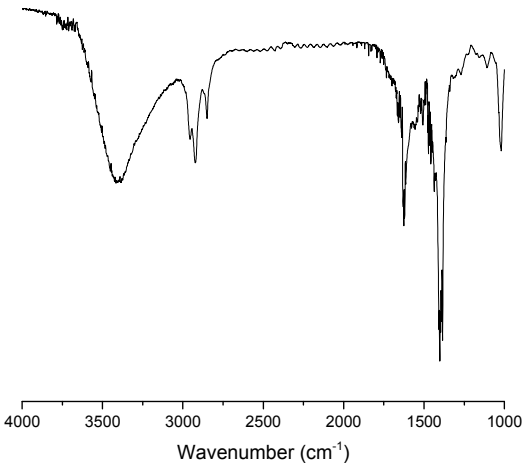

Figure S10. Zeta potentials of MIL-101(Cr)-QDMEN and MIL-101(Cr) at the presence of NaH_2PO_4buffer (2 mM).

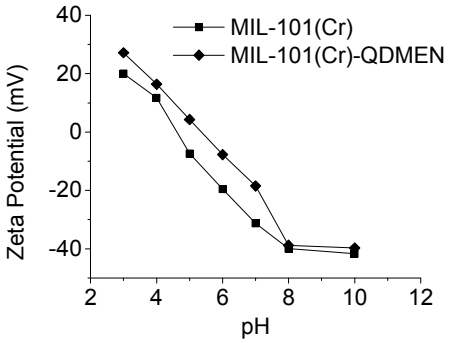

Figure S11. Optimized adsorption complex (AC) configurations for PFOA on pristine MIL-101(Cr).

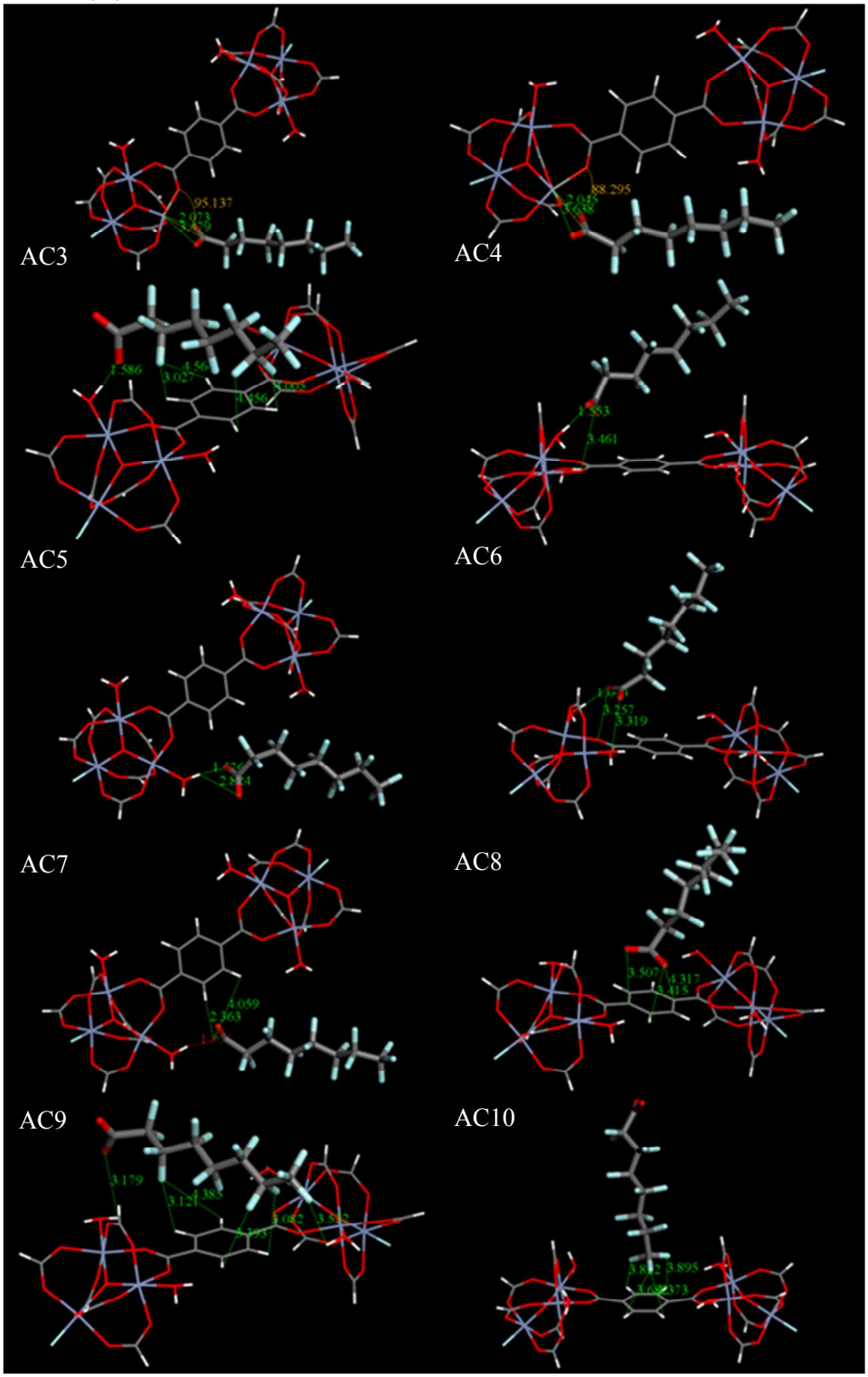

Figure S12. Optimized adsorption complex (AC) configurations for PFOA (stick) on protonated MIL-101(Cr).

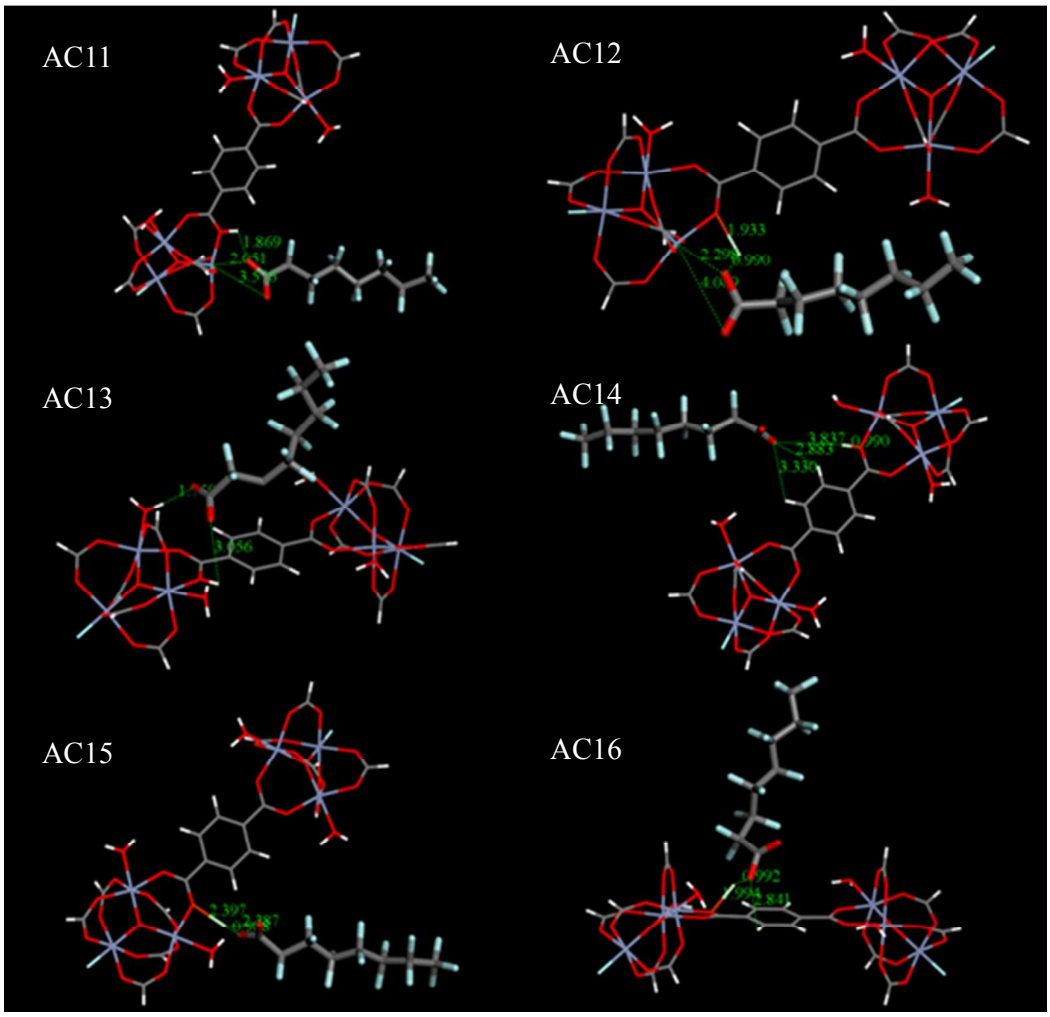

Figure S13. Optimized adsorption complex (AC) configurations for PFOA (stick) on MIL-101(Cr)-NH_2 (AC17, 18),MIL-101(Cr)-NMe_3(AC19, 20), MIL-101(Cr)-DMEN (AC21, 22), and MIL-101(Cr)-QDMEN (AC23, 24).